5. Evaluation of Graft Pretension Effects in an In Vivo Porcine Model

5.1 Introduction

During anterior cruciate ligament (ACL) reconstruction, various factors affect the outcome of the procedure. However, due to the complex biological system, these effects are not clearly understood. This study attempts to clarify the issues surrounding one potentially important variable in the surgery: graft pretension.

Researchers have demonstrated the importance of graft pretension using in vitro models [6,8,12,13,16,17,19]. But, in vitro studies only offer a glimpse at how the graft behaves at the instant of implantation. Because the graft is a living tissue that remodels over time in a process described as "ligamentization" [1,2,21], subsequent graft behavior can not be predicted using these models.

Few studies have examined the effects of graft pretension on the remodeling process. Yoshiya et al. [25] demonstrated a higher initial tension led to graft degeneration. No statistically significant differences in knee laxity or structural properties were attributed to graft pretension. The current study attempted to verify their findings and further examined the effects of pretension on histological, biochemical, and mechanical properties of grafts, which are indicators of tissue remodeling.

The load carried by a ligament or tendon has been suggested to affect tissue remodeling [20,22]. However, in vivo ACL graft forces have been examined only in a limited manner. Lewis et al. [14,15] measured graft forces with buckle transducers in an in vivo goat model. These studies are limited because the researchers implanted a ligament augmentation device to carry a portion of the graft load. Loads experienced during the healing phase by grafts implanted without this device may be markedly different than those with the augmentation. Because an augmentation device is not commonly used, conclusions made in these studies are limited in application. One purpose of this study was to investigate in vivo ACL graft forces using a more popular graft, the bone-patellar tendon-bone complex [3,10].

The viscoelastic nature of graft tissues introduces another factor when considering the question, To what extent should the graft be pretensioned? Should the pretension be selected so that normal knee kinematics are restored immediately following surgery, even though this pretension may lead to graft loads large enough to cause tissue degeneration? Or, does stress relaxation cause the graft tension to drop to a given level regardless of pretension? If so, a pretension can be selected to protect the graft tissue from damage. Therefore, knowledge of the graft's in vivo stress relaxation behavior is important to understand.

One problem with studying stress relaxation in vivo is the need to measure graft load at frequent intervals to obtain an accurate representation of the behavior. Lewis et al. [14,15] measured graft load at two and three week intervals. Because most of the stress relaxation is expected to occur shortly after implantation, much of the behavior is not recorded when load is measured at intervals of this duration. Hence, another purpose of this study was to develop a procedure to permit graft load to be monitored continuously to fully document the stress relaxation behavior.

5.2 Materials and Methods

5.2.1 Load Cell/Telemetry System

To provide a means to measure graft load, a load cell attachment was designed (Figure 5.1). A stainless steel casing with external M14 x 1.75 threads and a 0.375 in. (9.5 mm) diameter through hole was manufactured to fix one end of a 500 N load cell (model ELF-TC13-500, Entran, Fairfield, NJ) to the tibia via a cap. A grooved, hollow stainless steel cylinder with an external diameter equal to the internal diameter of the casing was manufactured to connect the tibial end of the graft to the free end of the load cell. With the device in place, a load transferred through the graft was registered by the load cell.

To allow continuous monitoring of graft load in vivo, an FM transmitter (MicroStrain, Burlington, VT) was used to collect the signal from the load cell. A transmitter unit consisting of a 3.0 V regulator, an A/D converter, an amplifier, a digital low-pass filter, and a digital transmitter was powered by a 3.6 V hermetically sealed lithium battery (size C, Tadiran, Inc., Israel). The gain of the amplifier, the cutoff frequency of the filter, and the number of input channels are programmable by the user. Values selected for this study were 32, 20 Hz, and 3 channels, respectively. Sampling frequency is dependent on the cutoff frequency and the number of input channels. With the selected values, the sampling rate in this study was 9.01 Hz. The regulator was used for bridge excitation of the load cell. The analog signal from the load cell was converted to a digital signal, amplified, filtered, and transmitted to a receiver connected to the serial port of an IBM-compatible 486 DX personal computer. Load data was recorded in real-time in RS-232 format.

To protect the electronic components of the load cell/transmitter system from the harsh in vivo environment, all exposed parts were waterproofed. The load cell was a sealed model, and the 36 in. (914 mm) lead wires were encased in polyvinyl chloride tubing. The insertion point of the lead wires to the load cell was sealed with epoxy. After the lead wires and the battery were connected to the transmitter unit, medical grade elastomer (type MDX4-4210, Dow Corning) was used to

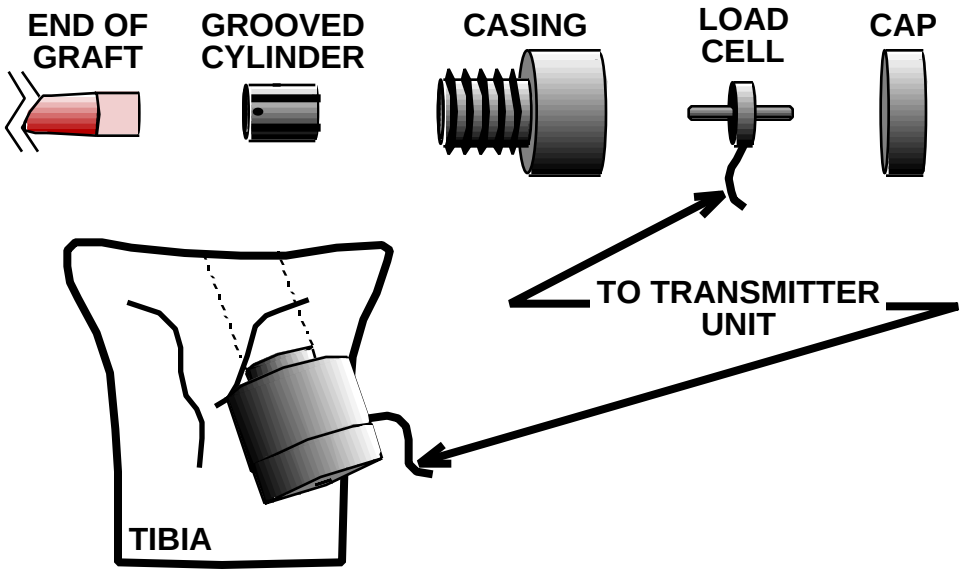

Figure 5.1 Load Cell Attachment

waterproof the components (Figure 5.2). Finally, a shell of poly(methyl methacrylate) was formed around the transmitter unit and battery to absorb impact forces (figure 5.3). The waterproofed load cell/telemetry system was sterilized with ethylene oxide gas prior to implantation.

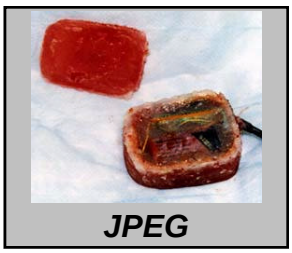

Press To View 75 dpi (19K)

Press To View 150 dpi (36K)

Press To View 300 dpi (98K)

Figure 5.2 Waterproofed Transmitter Unit and Battery

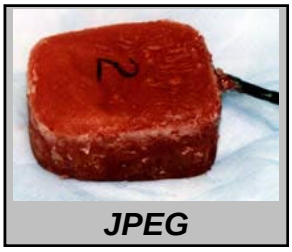

Press To View 75 dpi (15K)

Press To View 150 dpi (25K)

Press To View 300 dpi (59K)

Figure 5.3 Transmitter Unit Sealed in Poly(Methyl Methacrylate)

5.2.2 Animals

Five female pigs of the mini-Hanford breed (weight approximately 80 kg) were used in this study (Figure 5.4). Although limited in availability, only skeletally mature animals (age approximately 5 years) were obtained. If skeletally immature animals had been included, the healing process following surgery may have been affected because the reconstruction procedure required drilling through the area where the tibial growth plate would be found.

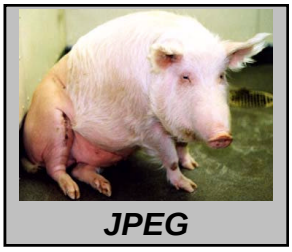

Press To View 75 dpi (22K)

Press To View 150 dpi (46K)

Press To View 300 dpi (110K)

Figure 5.4 Mini-Hanford Pig

5.2.3 Surgical Procedure

For 12 hours prior to surgery, food was withheld from the animal. Water was available during this period as desired. One hour prior to surgery, the animal was prepared for intubation and anesthesia. Intramuscular injections of 1.0 mg/kg acepromazine, 0.01 mg/kg glycopyrrolate, and 24 mg/kg ketamine were administered to act as a tranquilizer, a drying agent to aid intubation, and to induce anesthesia, respectively. The animal was then transferred to the operating table and intubated. Throughout the surgery, general anesthesia was maintained by isoflurane, and cefazolin sodium and buprenorphine hydrochloride were administered intravenously as a prophylactic antibiotic and an analgesic, respectively.

The right pelvic limb was shaved to the midline of the dorsal side. The shaved region was washed twice with a betadine solution and rinsed with 70% isopropyl alcohol and sterile 0.9% saline solution. The surgical field was then draped with sterile sheets (Figure 5.5).

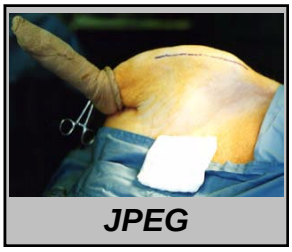

Figure 5.5 Prepared Surgical Field

The lateral half of the patellar tendon was harvested with sections of the patella and tibial tubercle as a 6 mm diameter graft (Figures 5.6, 5.7). The bone blocks were trimmed to size, and the tibial block was fixed in the grooved cylinder of the load cell connection using poly(methyl methacrylate) and two transverse 1.5 mm diameter Kirschner wires (Figure 5.8). TiCron sutures (size #5) were placed through the patellar block, and the graft was wrapped in saline soaked gauze until needed for implantation (Figure 5.9).

JPEG

Press To View 75 dpi (22K)

Press To View 150 dpi (41K)

Press To View 300 dpi (114K)

Figure 5.6 Isolating the Patellar Tendon Graft

JPEG

Press To View 75 dpi (16K)

Press To View 150 dpi (33K)

Press To View 300 dpi (111K)

Figure 5.7 Patellar Tendon Graft

JPEG

Press To View 75 dpi (19K)

Press To View 150 dpi (32K)

Press To View 300 dpi (81K)

Figure 5.8 Fixing the Graft in the Cylinder

JPEG

Press To View 75 dpi (10K)

Press To View 150 dpi (19K)

Press To View 300 dpi (41K)

Figure 5.9 Prepared Patellar Tendon Graft

The interior of the joint was visualized through a medial parapatellar incision. A 3.2 mm diameter Steinmann pin was inserted from the external tibial surface into the tibial insertion of the ACL to serve as a guide for drilling (Figure 5.10). The ACL was then transected and removed. A cannulated 1.25 in. (31.75 mm) diameter end mill was used to remove a portion of the tibia to provide room for the attachment of the load cell casing (Figure 5.11). A 12 mm diameter cannulated reamer was used to complete the hole through the tibia (Figure 5.12). The hole was prepared to receive the load cell casing using an M14 x 1.75 tap (Figure 5.13).

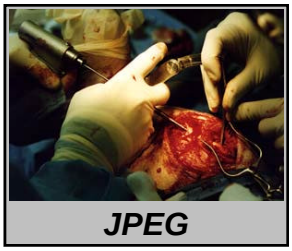

JPEG

Press To View 75 dpi (23K)

Press To View 150 dpi (45K)

Press To View 300 dpi (121K)

Figure 5.10 Inserting the Guide Pin

JPEG

Press To View 75 dpi (22K)

Press To View 150 dpi (40K)

Press To View 300 dpi (103K)

Figure 5.11 Removing a Portion of the Tibia

JPEG

Press To View 75 dpi (30K)

Press To View 150 dpi (63K)

Press To View 300 dpi (195K)

Figure 5.12 Reaming the Tibial Tunnel

JPEG

Press To View 75 dpi (18K)

Press To View 150 dpi (38K)

Press To View 300 dpi (79K)

Figure 5.13 Load Cell Casing in the Tibia

Using an offset rear entry positioning guide, a 3.2 mm diameter Steinmann pin was inserted through the femur at the location of the ACL insertion. A 10 mm diameter cannulated reamer was used to place a tunnel through the femur to receive the graft (Figure 5.14). An incision was placed on the dorsal side of the animal to insert the transmitter. The load cell and wires were passed subcutaneously from the dorsal incision to the limb incision so that the transmitter unit was positioned in the back and the load cell was near the tapped hole in the tibia (Figures 5.15-5.17).

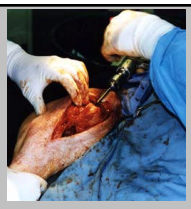

JPEG

Press To View 75 dpi (27K)

Press To View 150 dpi (53K)

Press To View 300 dpi (151K)

Figure 5.14 Reaming the Femoral Tunnel

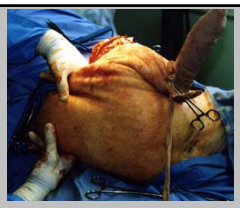

JPEG

Press To View 75 dpi (25K)

Press To View 150 dpi (48K)

Press To View 300 dpi (125K)

Figure 5.15 Passing the Load Cell Lead Wires Subcutaneously

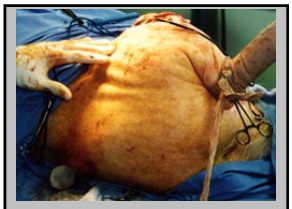

JPEG

Press To View 75 dpi (22K)

Press To View 150 dpi (41K)

Press To View 300 dpi (103K)

Figure 5.16 Transmitter Unit in Position After Passing the Lead Wires

JPEG

Press To View 75 dpi (17K)

Press To View 150 dpi (28K)

Press To View 300 dpi (64K)

Figure 5.17 Transmitter Unit Placed Subcutaneously

The graft was preconditioned by applying a constant 44.5 N tensile load for 15 min. Following the preconditioning period, the graft was connected to the load cell and, using the bone block sutures, was passed through the tibia to the femur (Figures 5.18-5.20). The load cell attachment was completed, and the knee was positioned at maximal extension (Figure 5.21). A 30 N (animal 1), 20 N (animals 2 and 4), or 10 N (animals 3 and 5) pretension was applied to the graft by a weight and pulley system via a sterile rope aligned with the femoral tunnel (Figure 5.22). An external fixator device was then fastened across the joint to maintain the resulting position. The graft was fixed in the femoral tunnel with a 9 mm interference screw (Figure 5.23). The incisions were closed using staples and subcutaneous #2-0 Vicryl sutures (Figures 5.24, 5.25). The knee was dressed with gauze sponges and wrapped with Coban elastic wrap.

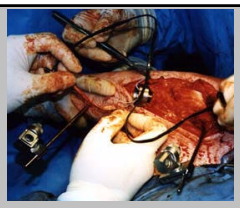

Figure 5.18 Passing the Graft, Start

Figure 5.19 Passing the Graft, Continued

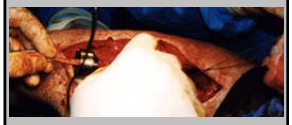

Figure 5.20 Passing the Graft, Continued

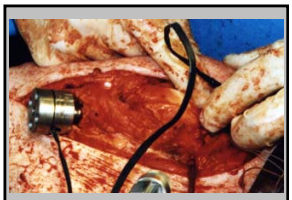

Figure 5.21 Completed Load Cell Attachment

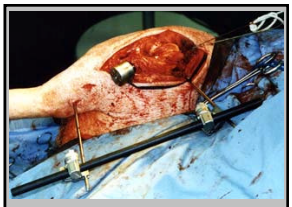

Figure 5.22 Pretensioning the Graft

Figure 5.23 Fixing the Graft in the Femoral Tunnel

Figure 5.24 Suturing the Incisions

Figure 5.25 Knee at Completion of Surgery

5.2.4 Post-Operative Animal Care

Following surgery, the animal was returned to the holding pen and observed until anesthesia effects subsided. The animal was then permitted normal cage activity as tolerated. Analgesics, anti-inflammatories, and antibiotics were administered as needed. Dietary consumption was monitored on a daily basis. Three to five weeks after the surgery, the animal was sacrificed by an intramuscular injection of 1.0 mg/kg acepromazine, followed by an intracardial injection of sodium pentobarbital.

5.2.5 Telemetric Data Collection

Telemetry data from the load cell was collected at several times throughout the study. First, graft load was recorded during application of the pretensioning weight and fixation of the graft to the femur. Second, graft load was recorded during the hour immediately following the surgery. Finally, graft load was recorded on a daily basis for intervals of approximately 15 min during animal activity and physical manipulation of the limb.

5.2.6 Tissue Analyses

Following sacrifice, the experimental graft and contralateral control patellar tendon and ACL were recovered for tissue analyses. After a gross inspection, the tissues were analyzed mechanically, biochemically, and histologically.

5.2.6.1 Mechanical Analysis

The experimental grafts were tested to determine mechanical characteristics. Mechanical characteristics of porcine patellar tendons determined in a prior study (see Chapter 4) were used as a control comparison.

5.2.6.1.1 Specimen Preparation

The experimental knees were isolated and dissected to leave only the femur-graft-tibia complex. The exposed tissue was kept moist throughout preparation and testing with a 0.9% saline spray. The tibia and femur were potted in sections of polyvinylchloride pipe with poly(methyl methacrylate).

5.2.6.1.2 Specimen Fixation

The specimens were loaded in a closed loop hydraulic testing machine (Model 1321, Instron, Canton, MA). Using a custom designed clamp, the femur was fixed to the base of the testing machine at an angle of approximately 60° to the vertical. This angle was selected to attempt uniform loading of most fibers in the tissue. The tibia was fixed vertically to the hydraulic actuator arm.

5.2.6.1.3 Cross-Sectional Area Determination

A rectangular cross-section was assumed to calculate cross-sectional area of the specimen. After application of a preload of approximately 1 N, width and depth at the mid-point of the specimen were measured three times each with digital calipers. The means of the measurements were used to calculate cross-sectional area.

5.2.6.1.4 Testing Protocol

A differential variable reluctance transducer (DVRT, MicroStrain, Burlington, VT) with a gauge length of 10 mm was inserted at the mid-point of the specimen to measure tissue strain [4]. The specimen was conditioned for 20 cycles with a 1.5 mm amplitude triangular wave at an elongation rate of 20 mm/min. The 1 N preload was again applied to the specimen before loading to failure at 200 mm/min. An A/D conversion board (Model Lab-NB, National Instruments, Austin, TX) and LabView 2 software (National Instruments) on a Macintosh LCIII computer were used to record load and DVRT data digitally.

5.2.6.1.5 Stress Relaxation Analysis

Stress relaxation during specimen conditioning was obtained from the load cell output. The level of cyclic stress relaxation was defined as the ratio of the peak load after equilibrium was reached to the peak load of the first cycle.

5.2.6.1.6 Stress-Strain Analysis

The stress-strain curve for each specimen was obtained from the stored digital data. Tissue stress was calculated from the load cell output and the initial cross-sectional area of the specimen. Tissue strain was calculated from the DVRT output and the initial transducer length. Ultimate stress, ultimate strain, and failure mode were noted. Ultimate stress was defined as the maximum value of stress attained during testing, and ultimate strain was defined as the strain at this point.

5.2.6.2 Histological Analysis

Following mechanical testing, a portion of each graft was imbedded in O.C.T. compound and frozen in preparation for histological analysis. Longitudinal and transverse sections (6 μm thickness) of an imbedded specimen were made using a Microtome Cryostat (MICROM, Germany). The sections were treated with hematoxylin and eosin biopsy stain to highlight tissue structure, which was compared to the control patellar tendon and ACL structures.

5.2.6.3 Biochemical Analysis

The remaining portion of each graft was analyzed biochemically following protocols described by Yin et al. [24] and Farndale et al. [7]. Water, collagen, DNA, and sulfated glycosaminoglycan contents were measured and compared to control patellar tendons and ACLs.

5.3 Results

5.3.1. Complications and Morbidity

A number of complications arose during the course of this study, thereby limiting the availability of information. Some complications prevented any form of data collection from an animal, while others merely limited the scope of the data.

5.3.1.1 Premature Graft Failure

The graft of the first animal failed during pretensioning (Figure 5.26). Therefore, data could not be collected, and the animal was sacrificed immediately. The cause of failure was probably due to

damage from excessive drying of the tissue. This issue was resolved for subsequent surgeries by carefully maintaining the graft in a saline moistened environment until implantation.

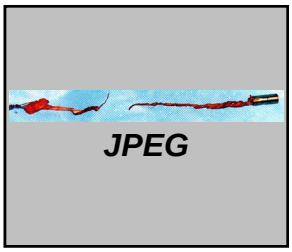

Press To View 75 dpi (15K)

Press To View 150 dpi (35K)

Press To View 300 dpi (79K)

Figure 5.26 Failed Graft from Animal 1

5.3.1.2 Infection

In addition to being laid open during the procedure, the surgical wounds were subjected to a decidedly non-sterile environment when the animal was returned to the holding pen. Food, dirt, feces, and urine were among the contaminants that were in contact with the wounds at some time. Hence, infection was a persistent possibility.

The second animal displayed the most significant infection, with approximately 10 ml of pus around the transmitter. Signs of the infection followed the lead wires to the load cell attachment. Tissue necrosis was noted in both areas (Figure 5.27). Progressively less infection was noted in each subsequent animal, until no signs of infection were seen in the fifth and final animal. Two possibilities exist to explain this improvement. First, the duration of the surgical procedure decreased with each ensuing animal as technique was improved with practice. This reduced the exposure of the underlying tissues to contaminants in the atmosphere. Second, prophylactic antibiotics were administered intravenously during the surgery of the fifth animal.

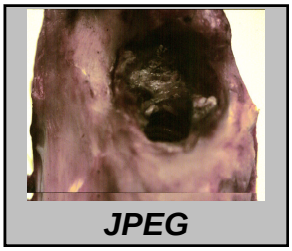

Press To View 256 dpi (18K)

Press To View 512 dpi (41K)

Press To View 1024 dpi (230K)

Figure 5.27 Tissue Necrosis Around Implant

5.3.1.3 Load Cell/Telemetry System

The load cell/telemetry system gave rise to several problems during the study. Because of these developments, graft load data was not available for the entire post-operative period for all animals. As with the reduction of infection, improvements were achieved with each subsequent animal.

The insertion point of the lead wires into the load cell proved to be fragile. This junction was broken when connecting the load cell to the graft in the second animal; hence, no graft load data was available for this animal. In subsequent animals, extra care was taken when making this connection.

Load data was successfully collected during the surgery of the third animal. However, the transmitted signal discontinued on post-operative day 1. After the full 4 week course of the experiment, recovery of the unit revealed waterproofing of the transmitter unit and battery had failed (Figure 5.28). It is believed that the medical grade elastomer had not fully cured before being subjected to the ethylene oxide sterilization process, and open pockets of air were formed. After this problem was realized, the medical grade elastomer was allowed to cure for 48 hours prior to sterilization. As additional fluid protection, the circuit board of the transmitter unit was factory-sealed in epoxy.

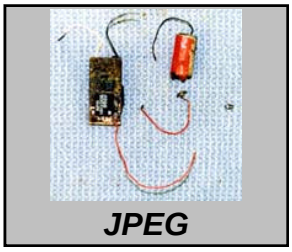

Figure 5.28 Fluid-Damaged Transmitter Unit

The transmitter unit itself failed in the fourth pig following 5 days of successful data collection. This failure was caused by the unit's power supply. In the first four animals, the unit was powered by a AA size battery. Due to the limited storage capacity of this battery, a magnetic reed switch was used to power down the unit when not collecting data. However, internal settings (e.g. amplifier gain and number of input channels) of the unit were apparently susceptible to the intermittent power supply and reset to unacceptable values. To eliminate this problem in the fifth animal, a size C battery capable of continuously powering the transmitter unit for 45 days was used, and the magnetic reed switch was removed. Using this setup, load data was collected for 23 post-operative days, until the junction of the lead wires at the load cell again broke. However, the issue of the changing internal settings remained unresolved. Based on calibrations prior to sterilization and prior to implantation, the gain of the amplifier was changed by the ethylene oxide sterilization process. New calibration factors were calibrated, but the gain apparently changed again on post-operative day 6. The cutoff frequency may also have changed. Because of this unexplained behavior, absolute graft loads from the fifth animal were difficult to interpret, although relative pattern descriptions are still valid.

5.3.2 Animal Activity

Activity following surgery was consistent from animal to animal. Over the first three post-operative days, the animals gradually learned to stand up and balance on three limbs (Figure 5.29). Slight to moderate weight bearing on the operated limb was noted, with greater loads occurring when an animal slipped. After this period, analgesic dosage was generally reduced, and the animals guarded the operated limb from any weight bearing (Figure 5.30). After approximately one to two weeks, the animals again began to use the operated limb for slight weight bearing, a behavior which continued until sacrifice. The effort to get up, balance, and walk appeared to be a more strenuous exertion than to which the animals were accustomed, and much of their time was passed recovering from these activities (Figure 5.31).

JPEG

Press To View 75 dpi (21K)

Press To View 150 dpi (46K)

Press To View 300 dpi (98K)

Figure 5.29 Animal Adapted to Operated Limb

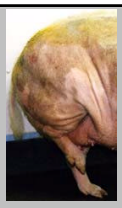

JPEG

Press To View 75 dpi (13K)

Press To View 150 dpi (23K)

Press To View 300 dpi (63K)

Figure 5.30 Animal Guarding Operated Limb

JPEG

Press To View 75 dpi (23K)

Press To View 150 dpi (56K)

Press To View 300 dpi (128K)

Figure 5.31 Animal Recovering from Activity

Food and liquid intake for all animals decreased following surgery. This fact, coupled with the presumed increase in caloric expenditure, lead to a weight loss of approximately 20% over the course of the experiment. The decreased appetite was possibly due to adverse effects of medications.

5.3.3 Graft Loads

The receiver proved capable of reading the signal from the implanted transmitter from a distance of up to 6 m. No disturbances due to the surrounding environment (e.g. metal fences) were noted.

During pretensioning, the indicated graft load was less than the applied force (Figure 5.32). This discrepancy is likely due to the oblique direction of the graft when compared with the axis of the load cell. Thus, only the component of graft load along the axis of the load cell was measured.

Inserting the interference screw consistently increased the load applied to the graft (Figure 5.32). Although it was inserted from the lateral side and directed toward the joint, the interference screw acted as an Archimedes screw mechanism and pulled the bone plug of the graft further into the femoral tunnel during fixation.

A minor amount of stress relaxation was noted in the one hour period following graft fixation. During this period, graft load typically decreased less than 5% of the peak load immediately following fixation.

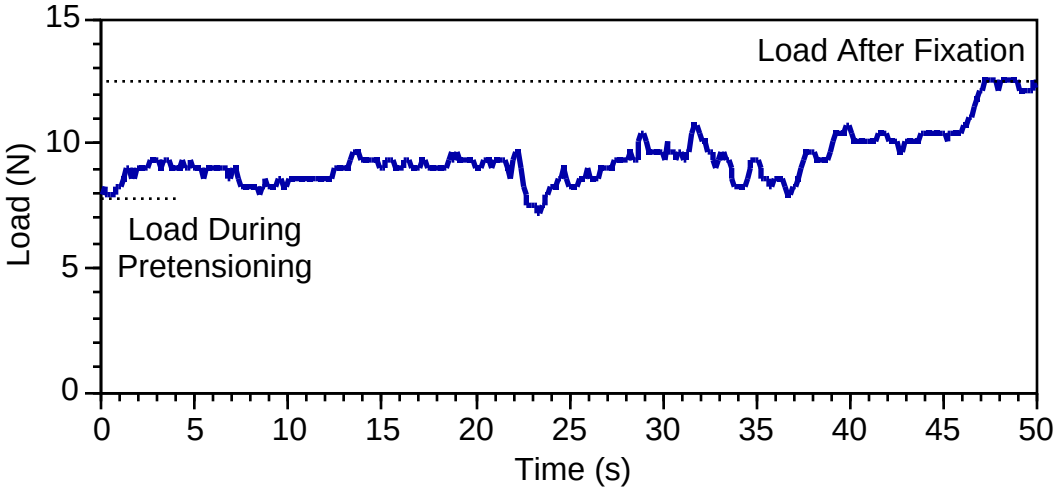

Figure 5.32 Graft Load During Interference Screw Fixation Following Pretensioning At 10 N

During passive joint motion, graft loads increased at high degrees of both flexion and extension (Figures 5.33, 5.34). Graft load was minimized in the middle of the flexion range. It is likely that the high degree of flexion possible in the pig (up to 170°) may cause impingement of the graft and hence development of a tensile force in the tissue. Passive abduction of the hip and knee, produced by applying a force to the hoof, also increased the graft load (Figure 5.35).

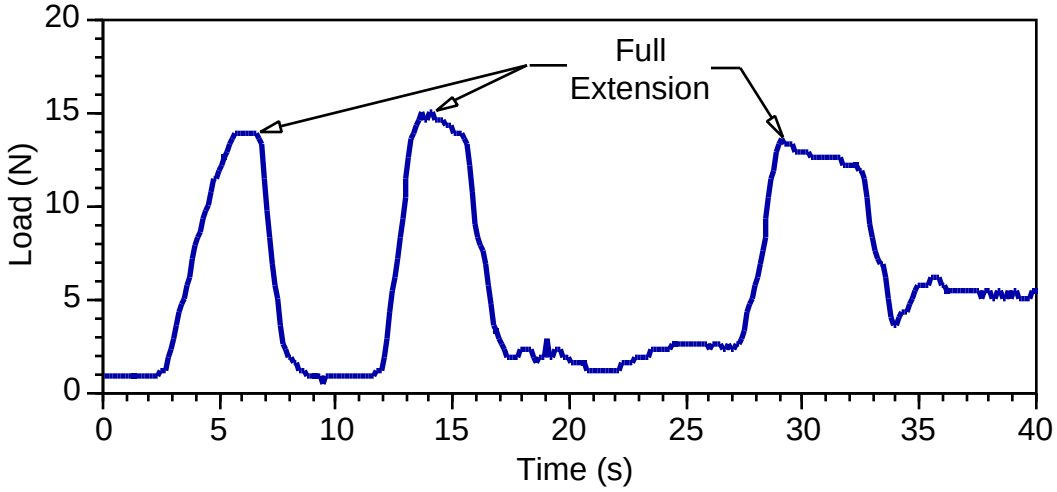

Figure 5.33 Graft Load During Cycles of Passive Extension of the Hip and Knee (Immediately Post-Op)

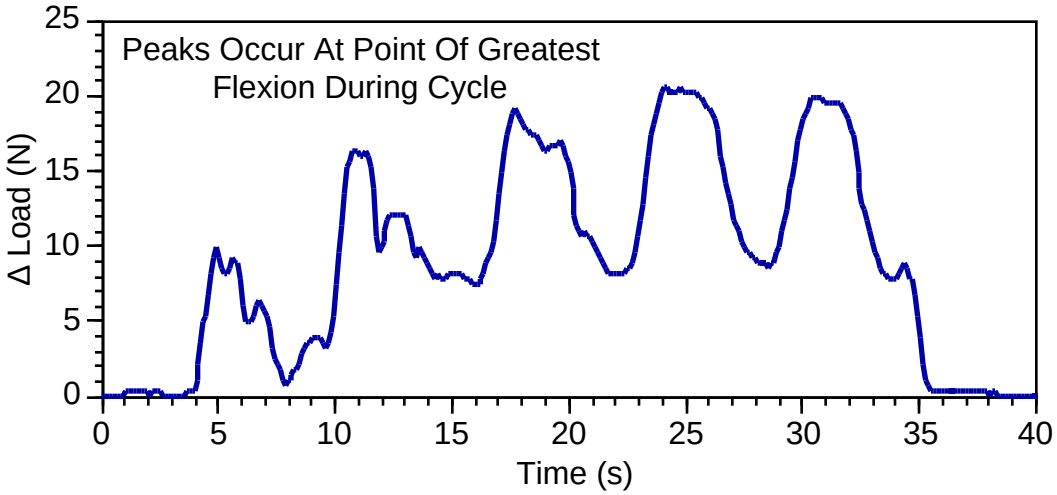

Figure 5.34 Change in Graft Load During Cycles of Passive Flexion of the Hip and Knee (Post-Op Day 2)

During active flexion of the hip and knee with no weight bearing, graft load increased (Figure 5.36). This increase may have been due to an active quadriceps force during the motion. A spike in graft load was seen during short periods of full weight bearing, as when the animal maneuvered from a reclining to a standing position. Following this spike, a curve reminiscent of tissue stress relaxation was noted, overlaid with relatively small increases in graft load when minimal weight was born on the limb (Figure 5.37).

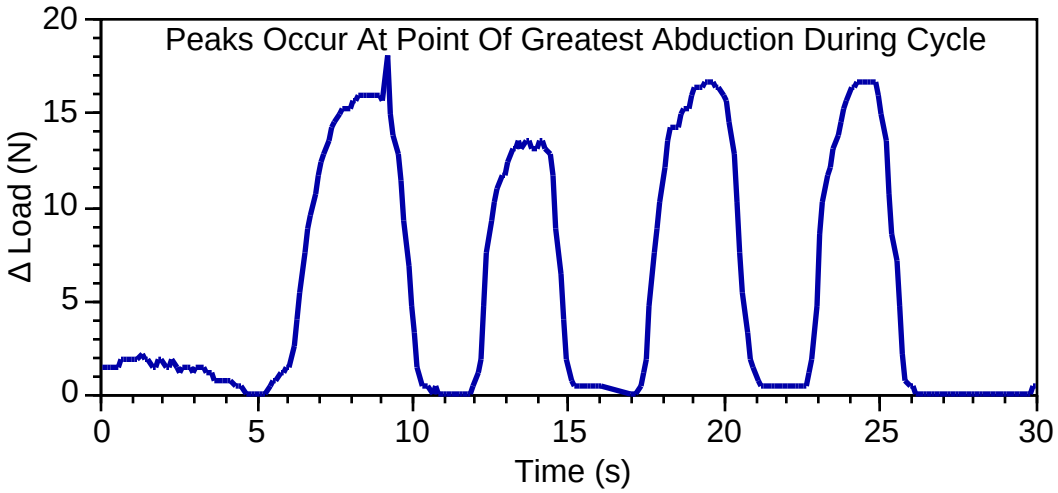

Figure 5.35 Change in Graft Load During Cycles of Passive Abduction of the Hip and Knee (Post-Op Day 2)

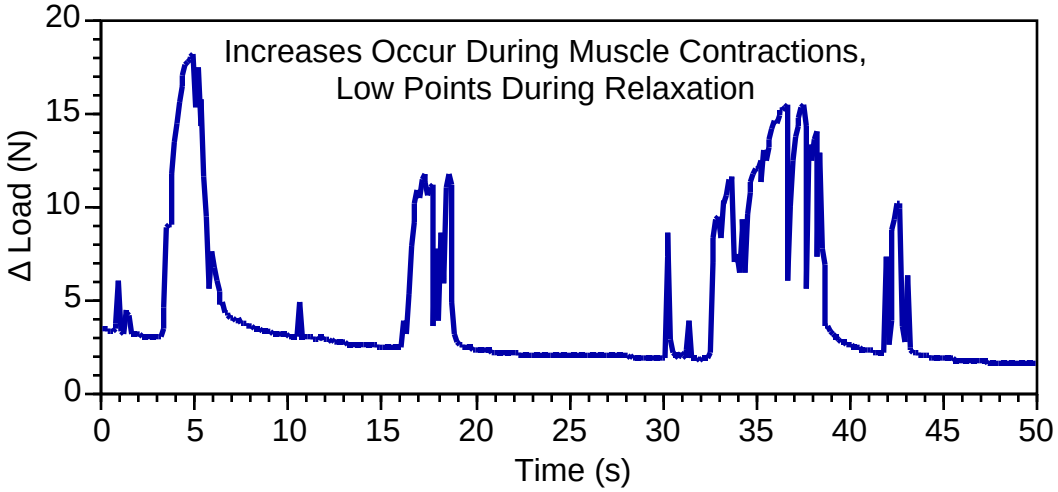

Figure 5.36 Change in Graft Load During Active Flexion of the Hip and Knee (Post-Op Day 9)

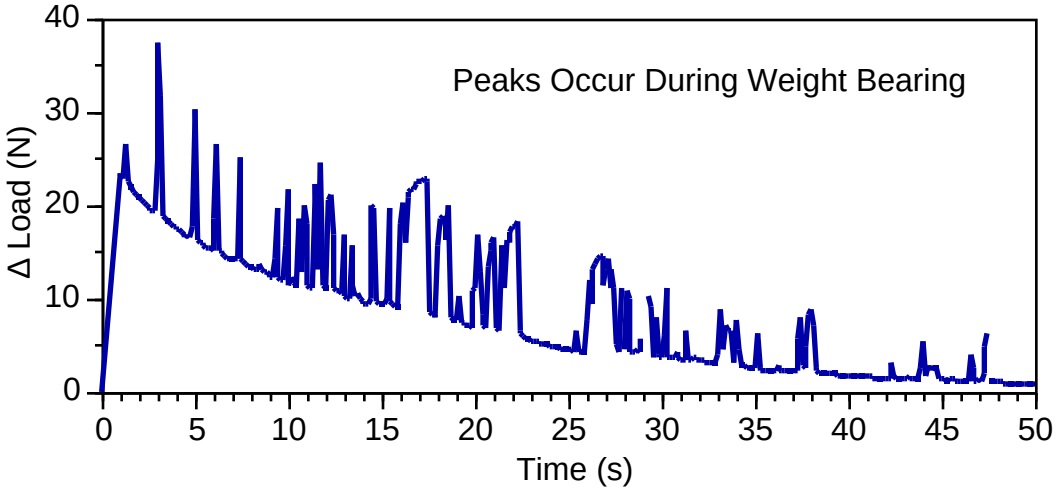

Figure 5.37 Change in Graft Load During Gait with Minimal Weight Bearing on Operated Limb (Post-Op Day 10)

5.3.4 Tissue Analyses

Gross inspection of control patellar tendons and ACLs revealed tissues that were white, glistening, and firm on palpitation. In contrast, the grafts appeared yellowish and somewhat edematous compared to the control tissues. Necrosis of the bony attachment of the graft in the grooved cylinder was apparent. There was formation of a new growth of unstructured tissue around the original patellar tendon structures. This tissue appeared to grow from the richly vascularized bone and to use the patellar tendon graft structure as a scaffolding. In animals 2 and 3, the tissue was attached between the anterior edge of the tibial tunnel and the femur. In animals 4 and 5, the tissue was contained entirely in and attached to the tibial tunnel. Capillaries were visible in the new tissue when viewed under the microscope.

5.3.4.1 Mechanical Analysis

Due to the newly formed tissue, the cross-sectional area varied greatly along the length of a graft. Because a graft typically failed at a location other than where the cross-sectional area was determined, values of ultimate stress should be viewed cautiously. Furthermore, a graft typically failed at a location outside of the DVRT. Hence, values of ultimate strain should also be viewed cautiously. With these limitations in mind, it can be summarized that all grafts displayed mechanical properties that were significantly lower than those of the control patellar tendons, with the possible exception of ultimate strain. Because the grafts from each animal were structurally different from one another, the results in this section are presented animal by animal.

5.3.4.1.1 Animal 2

The original patellar tendon structure of the graft from animal 2 broke during harvesting. Therefore, only the newly formed tissue from this animal was mechanically tested (Figure 5.38). Cross-sectional area was 44.1 mm^2. Peak load during cyclic conditioning relaxed to 68% of the initial peak load. The tissue failed at the insertion site of the tibia at a stress of 2.7 MPa. Because the barbs of the DVRT did not sufficiently grip the tissue, strain could not be determined for this specimen.

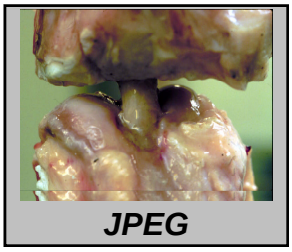

Figure 5.38 Graft from Animal 2

5.3.4.1.2 Animal 3

The original patellar tendon structure and the newly formed tissue of the graft from animal 3 were mechanically tested as a single unit (Figure 5.39). The cross-sectional area was determined, and the DVRT was inserted into the newly formed tissue. Cross-sectional area was 48.9 mm^2. Peak load during cyclic conditioning relaxed to 72% of the initial peak load. The tissues failed at the insertion site of the tibia at a stress of 2.0 MPa and a strain of 13% (Figure 5.40).

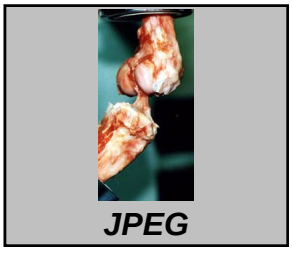

Figure 5.39 Graft from Animal 3

5.3.4.1.3 Animal 4

Because the DVRT did not fit in the space between the femur and tibia, the grooved cylinder was removed and gripped for testing the graft from animal 4 (Figure 5.41). The original patellar tendon structure and the newly formed tissue appeared in series. The cross-sectional area was determined, and the DVRT was inserted into the original patellar tendon structure. Cross-sectional area was 10.38 mm^2. Peak load during cyclic conditioning relaxed to 70% of the initial peak load. The graft failed by pulling free from the grooved cylinder at a stress of 4.0 MPa. No strain was indicated by the DVRT.

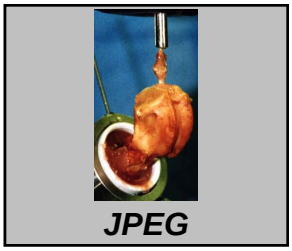

Press To View 150 dpi (19K)

Press To View 300 dpi (42K)

Press To View 600 dpi (94K)

Figure 5.41 Graft from Animal 4

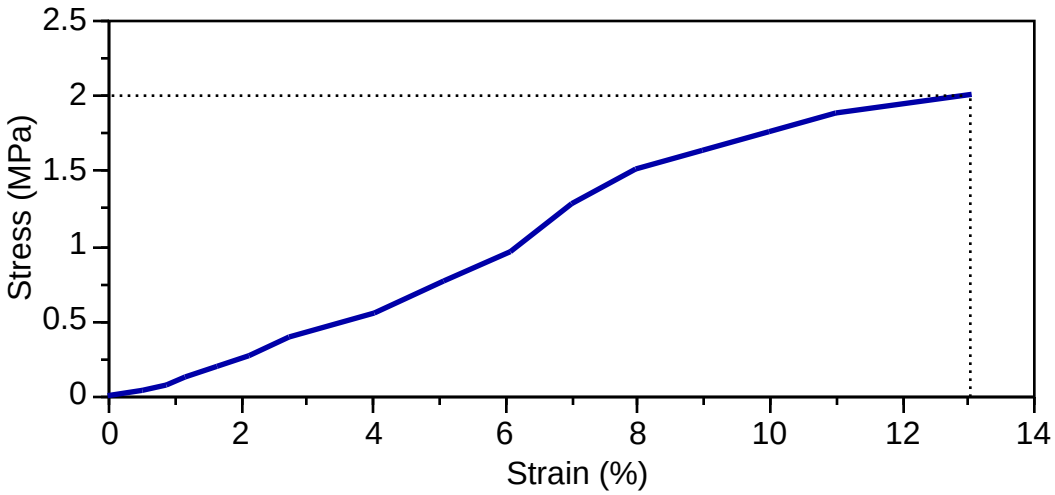

Figure 5.40 Stress-Strain Curve for Graft from Animal 3

5.3.4.1.4 Animal 5

The graft from animal 5 appeared to be a remodeled form of the original patellar tendon firmly attached to the femur and tibia (Figure 5.42). The cross-sectional area was determined, and the DVRT was inserted into the midpoint of the graft. Cross-sectional area was 41.1 mm^2. Peak load during cyclic conditioning relaxed to 67% of the initial peak load. The graft failed at a stress of 1.6 MPa and a strain of 6.2% in the midsubstance of tissue that pulled out from the femoral tunnel (Figure 5.43).

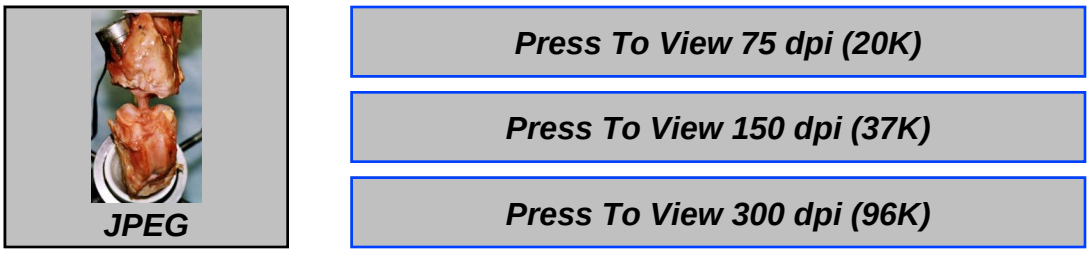

Figure 5.42 Graft from Animal 5

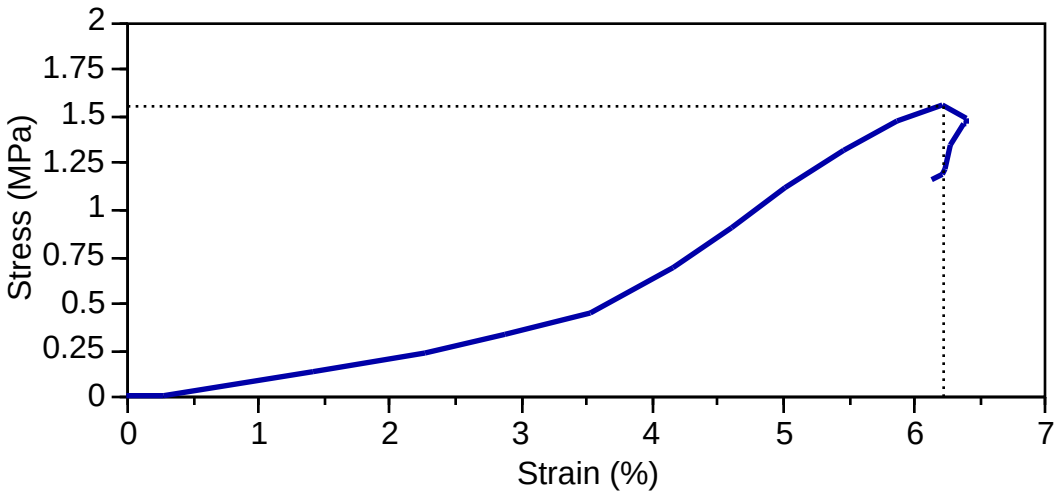

Figure 5.43 Stress-Strain Curve for Graft from Animal 5

5.3.4.2 Histological Analysis

Control patellar tendons displayed their typical profile: long and thin fibroblasts (20 ± 2 cells per view at 400x magnification), a low frequency crimp pattern of collagen fibers, and hypocellular matrix (Figure 5.44). Control ACLs displayed oval to spindle shaped fibroblasts (31 ± 3 cells per view at 400x magnification) and a high frequency crimp pattern of collagen fibers (Figures 5.45, 5.46). All of the grafts, however, showed a different profile: an irregular orientation of collagen fibers, an increased number of fibroblasts with plump oblong or oval shapes, and hypervascular extracellular matrix (Figures 5.47, 5.48). Compared to grafts pretensioned to 10 N, the grafts with a 20 N pretension had more fibroblasts (51 ± 3 versus 37 ± 2 cells per field at 400x magnification), larger fibroblasts, and more orderly orientation of collagen fibers. The new growth tissue appeared similar to granulated tissues, with hypercellular (74 ± 5 cells per filed at 400x magnification) and hypervascular extracellular matrix (Figures 5.49, 5.50). Figure 5.51 shows an insertion site section where ingrowth from the bone tunnel adhered to the graft tissue. Such ingrowth was seen in all grafts at the time of sacrifice.

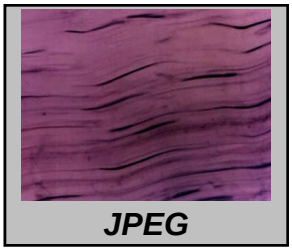

Figure 5.44 Longitudinal Section of Patellar Tendon (400x)

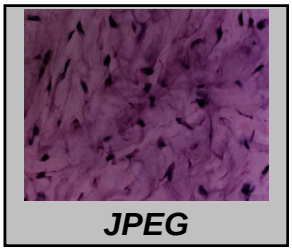

Figure 5.45 Longitudinal Section of Anterior Cruciate Ligament (400x)

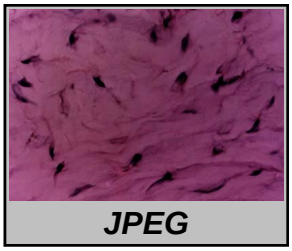

Figure 5.46 Cross Section of Anterior Cruciate Ligament (400x)

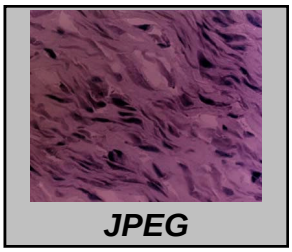

Figure 5.47 Longitudinal Section of Graft Pretensioned to 10 N (400x)

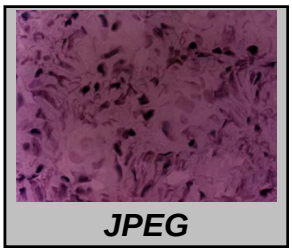

Figure 5.48 Cross Section of Graft Pretensioned to 10 N (400x)

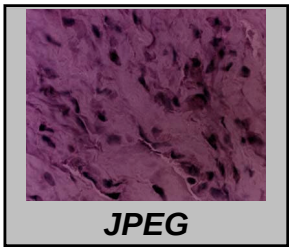

Figure 5.49 Longitudinal Section of New Growth (400x)

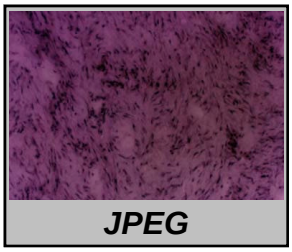

Figure 5.50 Cross Section of New Growth (100x)

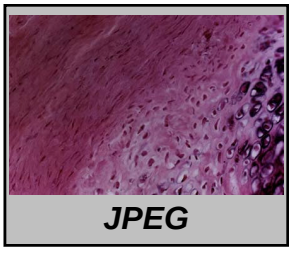

Figure 5.51 Section Showing Insertion Site of Graft in Tibia (200x)

5.3.4.3 Biochemical Analysis

The results of the biochemical analysis of control and experimental tissues are presented in Table 5.1. There were clear differences between control patellar tendons and ACLs for all measurements. Differences also existed between the control patellar tendons and grafts, but no differences were seen between the control ACLs and grafts. Differences also existed between grafts pretensioned at 10 N and those pretensioned at 20 N; the grafts pretensioned at 20 N were more similar to the control ACLs, thus indicating an enhanced ligamentization response.

Table 5.1 Summary of Biochemical Analysis of Control Tissues and Grafts

Tissue Type	Water Content[a]	Wet:Dry Ratio[b]	DNA Content[c]	Collagen Content[d]	Type-I Collagen[e]	s-GAG Content[f]
Patellar Tendon	66.0 ± 1.7	2.96 ± 0.15	1.532 ± 0.079	841 ± 14	95.4 ± 1.0	1.705 ± 0.149
ACL	73.5 ± 1.9	3.84 ± 0.30	2.69 ± 0.14	793 ± 9	91.0 ± 1.0	7.38 ± 0.16
Grafts (10 N Pretension)	70.4 ± 2.4	3.41 ± 0.27	2.91 ± 0.10	807 ± 17	93.1 ± 1.6	7.86 ± 0.15
Grafts (20 N Pretension)	73.1 ± 3.7	3.80 ± 0.52	2.85 ± 0.14	784 ± 17	91.3 ± 1.5	8.33 ± 0.35

Note: Values are mean ± standard error of the mean.

[a]% of blotted wet tissues; [b]ratio of wet to dry tissue weight; [c]mg/g dry tissue weight ; [d]mg/g dry tissue weight; [e]type I collagen as % of total collagen weight; [f]sulfated glycosaminoglycan, µg/mg dry tissue weight.

5.4 Discussion

To attain the goals of this study, a device was developed to monitor in vivo graft load in a non-invasive manner following ACL reconstruction with a bone-patellar tendon-bone graft. The device is capable of recording the load history of the graft for an extended period of time, up to the point when ingrowth from the bone tunnel reduces the force transferred to the load cell. Reconstructions were performed using the device with either a relatively low or moderate pretension to investigate potential differences in graft load history and tissue properties. Through the course of this study, several obstacles inherent to working with an in vivo environment were addressed.

A previously unreported finding with clinical relevance is the increase in graft load noted during interference screw fixation. Thus, a graft may be placed under a greater load than is intended, and damage to the tissue may result. While the pull-out strength of various methods of graft fixation has been investigated [11,18], the effect of these methods on graft load has not been addressed and

warrants further examination. It should be noted that the technique used to position the joint during pretensioning of the graft may play a significant role in the eventual graft load. For example, during an early operation in this study, an external fixator was not used. Instead, the joint was manually held at full extension by the hoof. When force was applied to the screwdriver with each turn of the interference screw, and hence applied to the femur, the joint was driven to hyperextension. In this case, graft load increased 240% during fixation. When the external fixator was used to control joint position, much smaller increases in graft load (56%), which can be directly attributed to fixation technique, were noted.

The role of the ACL or graft in controlling joint kinematics during the stance phase of gait is uncertain. While the observations of Brand [5] and Pope et al. [23] suggest that knee stability is provided primarily by joint geometry and structure, Holden et al. [9] reported consistent loading of the ACL during the stance phase. The current study supports the latter finding. Taking the relatively slow gait of the animals into account, measured graft loads were similar to those reported by Holden et al. for ACL load during the stance phase in walking goats.

Few studies in the literature have evaluated the effects of pretension on the remodeling process of ACL grafts. First, Amiel et al. [1] investigated histological and biochemical responses to a single pretension in a rabbit model and noted a ligamentization phenomenon. The current study found similar results using a porcine model and two pretension levels. Second, Yoshiya et al. [25] examined the effects of two pretension levels on the mechanical properties, histology, and vascularity of grafts in a canine model. No significant differences in mechanical properties were attributable to pretension, a finding supported by the current study. However, grafts that were pretensioned to a higher level (39 N) had poor vascularity and more disordered collagen fibers than grafts pretensioned to a lower level (1 N). In contrast, the current study found greater collagen fiber order in grafts pretensioned to 20 N than in those pretensioned to 10 N. Hence, it seems likely that an upper limit for pretensions exists, above which may lead to a more disorganized tissue. Selecting a pretension that is low (e.g. 1 N) does not appear to be as detrimental to the ligamentization process as a pretension that is high. Furthermore, within the preferred region, it may be hypothesized that a single pretension may be found to maximize the ligamentization process.

This study showed that a 20 N pretension on a porcine patellar tendon graft produced a remodeled tissue with histological and biochemical characteristics more similar to the intrinsic ACL than did grafts with a 10 N pretension. Hence, while a given pretension may best restore intact joint kinematics to an ACL-deficient knee, it may be more advantageous to select a pretension that better remodels the graft into a ligamentous tissue.